

Transmission needs across a fully renewable European power system



Rolando A. Rodríguez^{b,*}, Sarah Becker^c, Gorm B. Andresen^a, Dominik Heide^d,
Martin Greiner^{a,b}

^a Department of Engineering, Aarhus University, Ny Munkegade 118, 8000 Aarhus C, Denmark

^b Department of Mathematics, Aarhus University, Ny Munkegade 118, 8000 Aarhus C, Denmark

^c Frankfurt Institute for Advanced Studies (FIAS), Johann Wolfgang Goethe Universität, Ruth-Moufang-Straße 1, 60438 Frankfurt am Main, Germany

^d Deutsches Zentrum für Luft- und Raumfahrt (DLR), Pfaffenwaldring 38–40, 70569 Stuttgart, Germany

ARTICLE INFO

Article history:

Received 4 February 2013

Accepted 1 October 2013

Available online 23 October 2013

Keywords:

Renewable energy system

Power transmission

Constrained power flow

Wind power generation

Solar power generation

Large-scale integration

ABSTRACT

The residual load and excess power generation of 30 European countries with a 100% penetration of variable renewable energy sources are explored in order to quantify the benefit of power transmission between countries. Estimates are based on extensive weather data, which allows for modelling of hourly mismatches between the demand and renewable generation from wind and solar photovoltaics. For separated countries, balancing is required to cover around 24% of the total annual electricity consumption. This number can be reduced down to 15% once all countries are networked together with unconstrained interconnectors. The reduction represents the maximum possible benefit of transmission for the countries. The total Net Transfer Capacity of the unconstrained interconnectors is roughly 11.5 times larger than current values. However, constrained interconnector capacities 5.7 times larger than the current values are found to provide 98% of the maximum possible benefit of transmission. This motivates a detailed investigation of several constrained transmission capacity layouts to determine the export and import capabilities of countries participating in a fully renewable European electricity system.

© 2013 Elsevier Ltd. All rights reserved.

1. Introduction

The sustainability of the world's energy supply is strongly dependent on the successful integration of renewable sources. Variable Renewable Energy Sources (VRES), such as wind and solar energy, promise to be key elements in future energy systems [1–5]. The nature of VRES makes them hard to integrate into an electrical system that was built on more or less predictable loads with dispatchable generation. In small penetrations, the variations can be absorbed without much consequence, but will be harder to ignore in a future, highly renewable, macro energy system. The spatio-temporal dispersion of the weather patterns that define the output of wind and solar energy will lead to fluctuating mismatches between regional demand for and generation of electricity. This will give rise to new challenges for countries with a high penetration of VRES, such as the need for back-up conventional balancing, flexible demand, dispatchable renewable sources such as hydroelectric reservoirs or biomass, increased transmission capacities to neighbouring regions and energy storage [2,4]. In order to understand and to design the future energy systems with dominant shares of VRES, we need to let the weather decide.

For the optimal integration of VRES in future 100% renewable electricity systems, one wishes to make as much use as possible of renewables while minimizing the need for conventional balancing, both in the installed power capacity required and the energy expended [6]. Additionally, we wish to minimize the need for storage [7,8] and transmission capacities [9,10]. In determining lower bounds on the need for storage and transmission, the synergies between these factors and the need for balancing must be well understood [11,12]. In this article, we focus on determining the synergy between transmission and balancing.

There is a conflict between the need for maximizing the integration of fluctuating VRES and minimizing the expansion of the transmission system. Several studies have assessed the need for a larger transmission network [4,13–15]. Despite the planned investments in grid strength, the European Network of Transmission System Operators for Electricity (ENTSO-E) has identified 100 bottlenecks in their network development plan [16], with 80% of them due to integration of renewables. By looking at characteristic weather patterns and possible wind and solar power generation across Europe, potential transmission between regions has been estimated. This has been done for Germany [17], and with an economic approach for Europe [9,12]. A similar study has looked at regional aggregation and transmission in the United States [18]. Estimates on the size of an ideal transmission grid are large, such as

* Corresponding author.

E-mail address: rar@imf.au.dk (R.A. Rodríguez).

20 GW for the link between France and Spain [15], which is over 15 times larger than the current interconnector capacity.

Starting from the same large weather database as presented in Refs. [7,8,11], we estimate the potential output of wind and solar photovoltaic energy for any given country in a 30-node representation of Europe. In Section 2, we introduce a model which calculates the local mismatches between VRES generation and load in this set of interconnected countries, and which distributes the excess generation in a way that maximizes the use of renewables. An efficient usage of renewables also minimizes the need for balancing energy E coming from conventional dispatchable resources. Section 2 also explains how this optimal distribution of VRES excess generation can be found by performing a novel generalization of DC power flow calculations with constrained interconnectors. It also determines the interplay between installed transmission capacity and the benefit coming from transmission. In Section 3, the DC power flow model is applied to the case of a future, 100% renewable Europe. A minimum E that each country can attain through an optimal mix of wind and solar is found, and then compared to that of a fully connected, unconstrained Europe. The total E resulting from this unconstrained flow leads to the maximum benefit of transmission, when countries can make the most use of the renewable excess generation of their neighbours. By applying the constrained DC power flow calculation we find a precise relation between the installed transmission capacity and the required total balancing energy E . Section 4 discusses the limits to import and export capabilities, and the reduction of conventional power capacities. The conclusion is presented in Section 5.

2. Methodology

The following is a method to determine power flows in a power system with a large amount of VRES generation, and the benefit they bring by reducing the need for balancing. Power flow calculations are detailed for unconstrained and constrained cases.

2.1. Definitions

For a node n representing a country, the hourly VRES generation and the electrical load will generally not be equal. The hourly mismatch between the load L_n and the combined output of wind G_n^W and solar G_n^S generation in a 100% renewable system is defined as [7]

$$\Delta_n(t) = \left(\alpha_n^W \frac{G_n^W(t)}{\langle G_n^W(t) \rangle} + (1 - \alpha_n^W) \frac{G_n^S(t)}{\langle G_n^S(t) \rangle} \right) \cdot \langle L_n(t) \rangle - L_n(t). \quad (1)$$

Here, t represents the hourly timestep and α_n^W the wind share at node n . Time-averaged means are denoted by $\langle \cdot \rangle$. The VRES generation is normalized to its mean and scaled to the mean value of the load. Under this scaling, VRES generate as much energy, on average, as is consumed by the load. The mean of the mismatch $\langle \Delta_n \rangle = 0$, but, due to the fluctuations of the generation and the load, $\Delta_n(t)$ will almost always be either positive in case of excess generation or negative in case of deficit generation.

The negative part of the mismatch defines the positive-valued residual load of a country,

$$\Delta_n^-(t) = \max\{-\Delta_n(t), 0\}, \quad (2)$$

which needs to be balanced by other dispatchable generation sources. The positive part of the mismatch is positive-valued excess power

$$\Delta_n^+(t) = \max\{\Delta_n(t), 0\}, \quad (3)$$

which must either be exported or curtailed. The time averages of (2) and (3) are identical, $\langle \Delta_n^- \rangle = \langle \Delta_n^+ \rangle$.

2.2. Unconstrained DC power flow

Assuming that the nodes are connected by links, the transmission of energy would follow Kirchhoff's rules for electric flow. Given a directed graph consisting of N nodes and L links with zero global mismatch, that is

$$\sum_{n=1}^N \Delta_n = 0, \quad (4)$$

the DC approximation to the full AC power flow [19] unambiguously defines the flow between two neighbouring nodes n and m as

$$F_{n \rightarrow m} = b_{nm}(\delta_n - \delta_m), \quad (5)$$

where b_{nm} is the susceptance of the connecting link and δ_n and δ_m are the voltage phase angles of the connected nodes n and m , respectively. The relative phase angles thus determine the potential flow between all nodes in the graph, and can be found by solving the system of N equations

$$\Delta_n = \sum_{m=1}^N B_{n,m} \delta_m. \quad (6)$$

The elements of the susceptance matrix B are defined by

$$B_{n,m} = \begin{cases} -b_{nm} & \text{if } n \neq m \\ \sum_{m \neq n}^N b_{nm} & \text{if } n = m \end{cases} \quad (7)$$

The DC approximation defined by (4), (5), and (6) is valid as long as the network is in steady state, the resistances of the links can be neglected and no significant voltage phase shifts occur between the nodes [20]. Another consequence of the zero-resistance assumption is that the susceptances do not depend on the length of the links and can be uniformly chosen to be equal to one. This means that the $N \times N$ matrix B becomes exactly identical to the matrix product of the $N \times L$ incidence matrix K ,

$$B = K \cdot K^T, \quad (8)$$

where K is

$$K_{n,l} = \begin{cases} 1 & \text{if link } l \text{ starts at node } n, \\ -1 & \text{if link } l \text{ ends at node } n, \\ 0 & \text{otherwise.} \end{cases} \quad (9)$$

Equations (5) and (6) can then be expressed as

$$F = K^T \cdot \delta \quad (10)$$

and

$$\Delta = K \cdot K^T \cdot \delta = K \cdot F. \quad (11)$$

The last equation expresses local flow conservation at each node.

The power flows (5) resulting from the DC power flow equations (4) and (6) can also be derived from the constrained quadratic minimization objective

$$\begin{aligned} \min_F F^T F \\ \text{s.t. } K \cdot F = \Delta. \end{aligned} \quad (12)$$

This can be shown by using a vector of N Lagrange multipliers λ to find the minimum of the constrained function

$$\Lambda = \frac{1}{2} F^T F - \lambda^T (KF - \Delta) \quad (13)$$

via

$$\frac{\partial \Lambda}{\partial F} = F^T - \lambda^T K = 0, \quad (14)$$

which leads to

$$F = K^T \lambda. \quad (15)$$

This last result has the same form as (10), meaning that the Lagrange multipliers λ can be interpreted as the voltage phase angles δ .

The two formulations (4)–(6) and (12) are fully equivalent. We will now use the second approach to generalize the unconstrained DC power flow to the dominating situation

$$\sum_{n=1}^N \Delta_n \neq 0,$$

when the combined mismatch of all nodes is not zero. In case of a negative sum, some nodes with a negative mismatch will not be able to import enough and will be required to balance the remainder from their own dispatchable sources:

$$B_n(t) = -\min \left\{ \left[\Delta_n(t) - \sum_{l=1}^L K_{n,l} F_l(t) \right], 0 \right\}. \quad (16)$$

Likewise, in case of an overall positive mismatch, some nodes will not be able to export all of their excess energy and will be required to curtail:

$$C_n(t) = \max \left\{ \left[\Delta_n(t) - \sum_{l=1}^L K_{n,l} F_l(t) \right], 0 \right\}. \quad (17)$$

By their definition, both B_n and C_n are positive at all times.

The balancing B_n , the excess energy C_n and the flows F_l at all nodes and links are now determined by a two-step optimization procedure. The first priority is the minimization of the overall balancing for each hour:

$$B_{\min}(t) = \min_{F_l} \sum_{n=1}^N B_n(t), \quad (18)$$

which guarantees a maximum usage of VRES across all nodes. Since this does not yet determine the flows in a unique manner, they are fixed in a second step,

$$\begin{aligned} \min_{F_l} \sum_{l=1}^L F_l^2 \\ \text{s.t. } \sum_{n=1}^N B_n = B_{\min}, \end{aligned} \quad (19)$$

which minimizes the quadratic flows with the constraint of keeping the total balancing at its minimal value found in the first step. The two steps ensure that we arrive at the most localized DC power flows which allow an optimal sharing of renewables between

exporters ($\Delta_n > 0$) and importers ($\Delta_n < 0$). The following constraints are implicitly fulfilled by the two-step optimization (18), (19):

$$\begin{aligned} \text{if } \Delta_n < 0, \quad \text{then } 0 \leq B_n \leq -\Delta_n \\ \text{if } \Delta_n > 0, \quad \text{then } 0 \leq C_n \leq \Delta_n; \end{aligned} \quad (20)$$

a violation would lead to additional flows, increasing the squared flow sum (19).

2.3. Constrained DC power flow

Today's transmission grids are constrained by the Net Transfer Capacities (NTC). These constraints are based not only on the physical properties of the interconnectors, the Total Transfer Capacities (TTC), but also on the strength of the grid on either sides of the link and on the security policies of the participating countries [21]. As a result, transmission over links is constrained with different values in each direction.

The problem, as stated in equation (19), can be further generalized by adding limits $f_l^- \leq F_l \leq f_l^+$:

$$\begin{aligned} \text{Step 1 : } \min_{F_l} \sum_{n=1}^N B_n &\equiv B_{\min} \\ \text{s.t. } f_l^- &\leq F_l \leq f_l^+ \\ \text{Step 2 : } \min_{F_l} \sum_{l=1}^L F_l^2 \\ \text{s.t. } f_l^- &\leq F_l \leq f_l^+ \\ \sum_{n=1}^N B_n &= B_{\min}. \end{aligned} \quad (21)$$

The first step can be solved linearly with the help of a slack variable, whereas the second step is a quadratic programming optimization problem. Solutions can be obtained with several computational solving tools. The high speed of the solvers generated by CVXGEN [22] made this tool well suited for our purposes.

2.4. Benefit of transmission

The constrained optimization (21) determines the power flows F_l on all links and, via (16), also the residual loads B_n on all nodes. It is important to note that the resulting power flows and residual loads depend on the transmission capacity layout $\{f_l^\pm\}$ that constrains the power flows. Each layout $\{f_l^\pm\}$ will result in a mean annual balancing energy

$$E = \frac{1}{Y} \sum_{t=1}^T \sum_{n=1}^N B_n(t) \quad (22)$$

which is the sum over all country-specific balancing needs at all times, divided by the number of years Y in the dataset of length T . The case of zero transmission capacity layout $f^\pm = 0$ results in zero power flows, so that the mean annual balancing energy

$$E(f_l^\pm = 0) = \frac{1}{Y} \sum_{t=1}^T \sum_{n=1}^N \Delta_n^-(t) \quad (23)$$

can be expressed as the country sum over the individual negative mismatches (2). Unconstrained power flows represent the other extreme and are the result of an infinitely strong layout. The resulting annual balancing energy

$$E(\infty) = \frac{1}{Y} \sum_{t=1}^T \max \left(- \sum_{n=1}^N \Delta_n(t), 0 \right) \quad (24)$$

can be obtained without a flow calculation, simply by allowing countries' mismatches to be summed before determining the amount of balancing required. Similarly, intermediate layouts $\{f_i^\pm\}$ between the two extremes will result in an annual balancing energy $E(\infty) \leq E(f_i^\pm) \leq E(0)$.

A measure on how much a transmission capacity layout is able to reduce the annual balancing energy is defined by the benefit of transmission

$$\beta = \frac{E(0) - E(\{f_i^\pm\})}{E(0) - E(\infty)}. \quad (25)$$

The benefit of the zero transmission is thus $\beta = 0$, and that of the unconstrained layout is $\beta = 1$. Intermediate layouts will result in $0 \leq \beta \leq 1$.

3. Case study: power transmission in a fully renewable Europe

The methodology developed in the previous section is applied to the case of a 30-node fully renewable European network. Each country is assumed to have a combined wind and solar power generation that is, on average, equal to its load. Country-specific optimal mixes are first determined. Then, the unconstrained formulation (19) for the power flow is used to estimate maximum transmission capacities on the interconnectors. Finally, the constrained power flow problem (21) is solved with different capacity layouts and the respective benefits of transmission β are determined.

3.1. Country specific optimal mixes

Focussing on wind and solar energy, VRES generation potentials were determined for 30 European countries from a large weather database, spanning eight years from 2000 to 2007 [7]. This includes both on- and off-shore regions with a spatial resolution of $47 \text{ km} \times 47 \text{ km}$. Weather measurements were used to determine wind and solar energy generation time series with an hourly resolution. To obtain the absolute power output for a country, capacity scaling factors were applied to each grid cell belonging to the country to be aggregated. The scaling factors reflect the assumed installed wind and solar capacity at that location. Historical data for the electricity demand was used to generate hourly load time series for all 30 countries covering the same 8 years from 2000 to 2007. The time series for each country were then detrended to correct for the approximately 2% annual increase in electricity demand. Average loads for the countries can be seen in Table 1.

The distribution of the mismatch is shown in Fig. 1 for three different countries, with three different choices for the mixing parameter ranging from fully solar ($\alpha_n^W = 0.0$) to fully wind ($\alpha_n^W = 1.0$). It is evident that the mismatch distributions depend on the mixing parameter α_n^W , and that no mix will completely eliminate the positive and negative mismatches. Our optimization objective is to minimize the average negative mismatch with respect to the wind share α_n^W . Since the average negative mismatch $\langle \Delta_n^-(t) \rangle = \langle \Delta_n^+(t) \rangle$ is identical to the average excess power, this is equivalent to the minimization of average excess generation. The optimal mixing parameters are shown in Fig. 2(a). Compared to the average optimal wind mix $\alpha_n^W \approx 0.71$, southern countries have a slightly smaller and northern countries a slightly larger value.

For an average country, the minimized average residual load amounts to 24% of its average load (see Fig. 2(b)). This implies that although the average wind and solar power generation are equal to the average load, 24% of it is generated at the wrong time. This amount has to be covered by dispatchable sources.

Table 1

Country specific average hourly load, detrended to their values for the year 2007.

ISO	Country	$\langle L \rangle$ (GW)	ISO	Country	$\langle L \rangle$ (GW)	ISO	Country	$\langle L \rangle$ (GW)
DE	Germany	54.2	FI	Finland	9.0	RS	Serbia	3.9
FR	France	51.1	CZ	Czech Republic	6.7	IE	Ireland	3.2
GB	Great Britain	38.5	AT	Austria	5.8	SK	Slovakia	3.1
IT	Italy	34.5	GR	Greece	5.8	BA	Bosnia & Herz.	3.1
ES	Spain	24.3	RO	Romania	5.4	HR	Croatia	1.6
SE	Sweden	16.6	BG	Bulgaria	5.1	LT	Lithuania	1.5
PL	Poland	15.2	PO	Portugal	4.8	EE	Estonia	1.4
NO	Norway	13.7	CH	Switzerland	4.8	SI	Slovenia	1.4
NL	Netherlands	11.5	HU	Hungary	4.4	LV	Latvia	0.7
BE	Belgium	9.5	DK	Denmark	3.9	LU	Luxembourg	0.7
						EU	Europe	345.5

The absolute values of the mismatch quantiles are shown in Fig. 2(c). Higher values in the quantiles imply larger deviations of VRES generation from the mean load. The 1% and 10% quantiles give an indication of the required balancing capacities resulting from the residual load time series defined by (2). The 90% and 99% quantiles are also shown and can be interpreted as the curtailed energy resulting from the excess time series defined by (3). Whereas the 90% quantiles are only a little larger than the 10% quantiles, the 99% quantiles turn out to be significantly larger than the 1% quantiles. For the larger fraction of the countries the 99% mismatch quantile is also larger than the 99% load quantile. These are the expected results when looking again at the asymmetry of the mismatch distributions of Fig. 1.

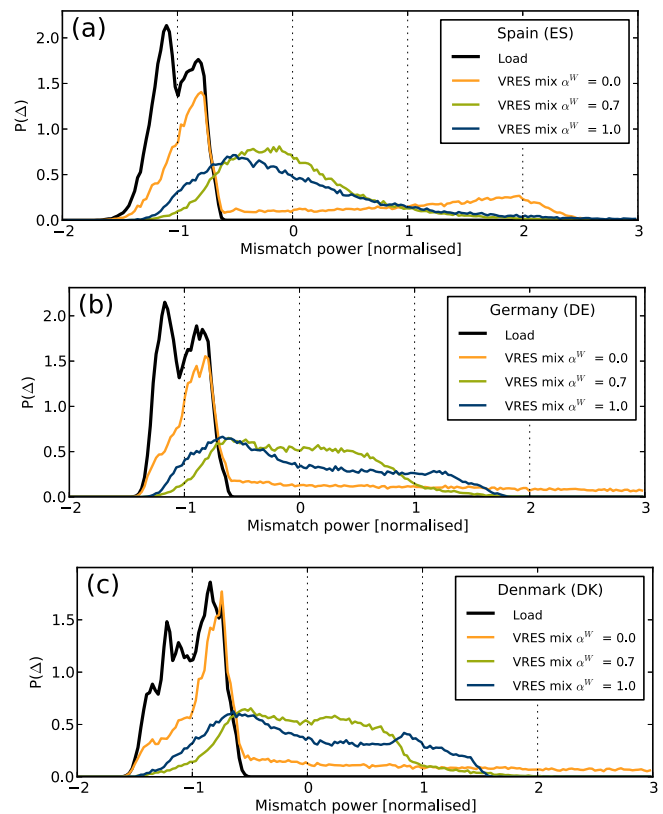


Fig. 1. Mismatch distributions for (a) Spain, (b) Germany and (c) Denmark with no cross-border transmission, for a fully renewable system. Values are normalized to the country specific mean load (see Table 1). The different colors represent the wind shares $\alpha_n^W = 0.0, 0.7, 1.0$. For comparison, the distribution of the normalized load is also shown.

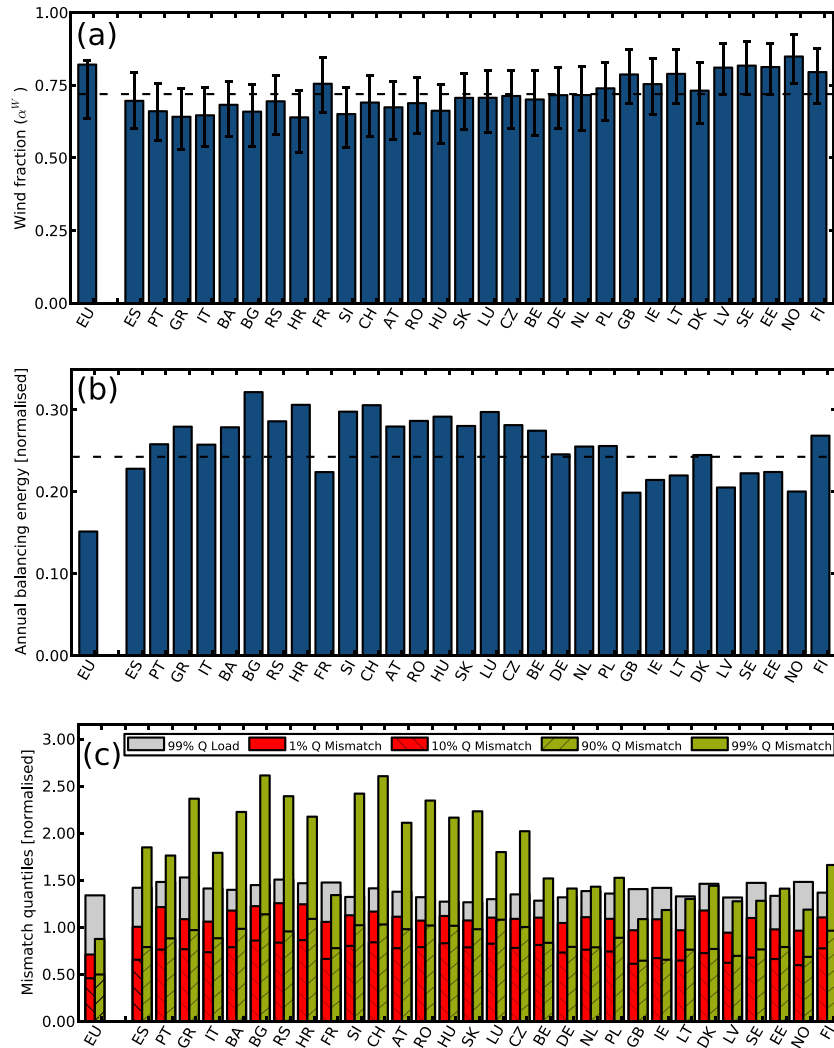


Fig. 2. (a) Optimal mix minimizing the average residual load calculated independently for each country and for aggregated Europe. Countries are ordered by the latitude of their geometric centre. Error bars show mixes that produce average residual loads which are larger by 1% compared to the optimum. The dashed line indicates the optimal mix averaged over all countries. (b) Minimum average residual load for each country, obtained with the optimal mixes from (a), in units of the country specific average hourly load (see Table 1). The dashed line indicates the residual load averaged over all countries. (c) The 1% (red), 10% (striped red), 90% (striped green), 99% (green) quantiles of the mismatch time series are based on the optimal mix from (a). As a reference the 99% quantiles (grey) of the load time series are also indicated. (For interpretation of the references to colour in this figure legend, the reader is referred to the web version of this article.)

We now compare the results for individual countries to those of the aggregated EU. The latter is assumed to have an unconstrained transmission between all countries, so that all excess generation can be shared with other countries. When each country has its optimal mix of renewables installed, the average residual load for all individual countries amounts to 24% of the average load, shown as the dotted line in Fig. 2(b). However, once all countries are aggregated, each with its own optimal mix, the resulting average residual load turns out to be $\langle \Delta_{EU} \rangle = 15\%$. This is in full agreement with the results found in Ref. [7]. This means that the largest reduction in its need for balancing energy that the average country can expect from its embedding into Europe is of the order of 40%, and sets an upper bound on what an ideal transmission system can do to reduce the need for balancing energy in Europe. While the Europe-wide optimal wind mix of $\alpha_{EU}^W = 0.82$ would result in smaller need for balancing, the bars showing mixes resulting in balancing energies within 1% of the minimum hint at a shallow optimum. For a more extensive discussion on country-specific optimal mixes, readers are directed to [23].

3.2. Unconstrained power flow

We now determine how much transmission capacity is needed for a layout to behave as though it was unconstrained. We apply the problem, as defined in equation (19), to a network representing 30 European countries and the links between them. The topology of the network is based on the layout reported by ENTSO-E for winter 2010–2011 [24], as well as from individual reports for links not found on ENTSO-E's report [25,26], and is initially assumed to have no capacity constraints; see Fig. 3.

Power flows and local balancing were calculated for every hour in the eight year span, assuming the country-specific optimal wind mixes α_n^W . The distribution of the resulting non-constrained power flow along a selected link is shown in Fig. 4. The maximum unconstrained power flow from France to Spain amounts to 38 GW, which is larger than the combined average loads of Spain and Portugal by a factor 1.3. In the other direction the maximum flow is 75 GW, which is 1.5 times the mean load in France.

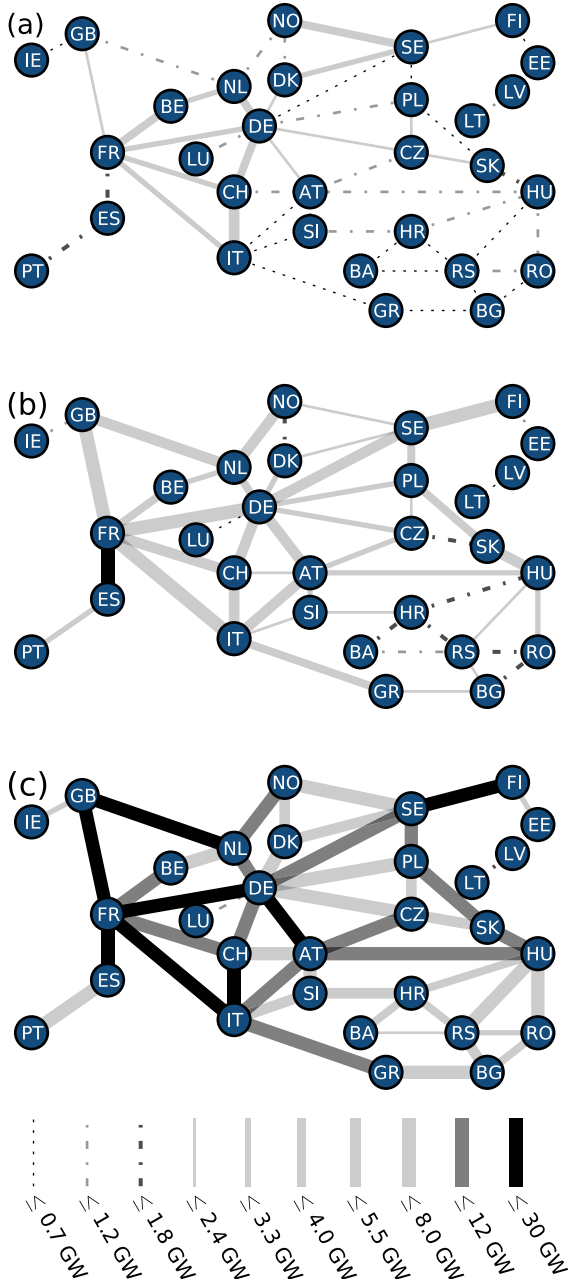


Fig. 3. Transmission network topology and link capacity, with the links as of 2012 [24–26]. (a) Present layout capacities. (b) Intermediate layout, with a total capacity 2.3 times larger. (c) 99% Quantile layout, with 5.7 times the total capacity of (a). All three layouts are described in detail in Table 3. Line thickness represents the larger NTC of the interconnector.

We define the Unconstrained layout as that in which all links have capacities equal to the maximum recorded exchange, so that power can flow unconstrained along the interconnectors. By construction, these give rise to the full benefit of cooperation, as they allow the interactions between countries to be identical to one in which they are all aggregated. The sum of the transmission capacities

$$T_C = \sum_{l=1}^L \max\{|f_l^-|, |f_l^+|\} \quad (26)$$

over the larger NTC value of each interconnector in the present layout adds up to around 73 GW. With 840 GW the Unconstrained

layout capacities are 11.5 times larger. These unconstrained capacities are determined by single, 1-h events over eight years of data. Therefore, we consider the 1% and 99% quantiles of the flow distributions to define a reduced, directed capacity layout, which we call the 99% Quantile layout; see again Fig. 4. This means that power will flow unobstructed for 98% of the time. The remaining 2% corresponds to around one week per year. The 99% Quantile layout comes with 395 GW in total and is roughly half as large as the Unconstrained layout, but still 5.7 times larger than today's interconnector capacities. See Table 3.

3.3. Constrained power flow

To determine what fraction of the benefit of transmission is obtained with a non-ideal, limited transmission capacity, we deal with constrained power flows as defined in (21). This allows the determination of a compromise between the reduction in balancing energy and the increase in total transmission capacity.

As can be seen in Table 2, the 99% quantile capacities provide, with $\beta = 97.6\%$, most of the benefit of the Unconstrained layout with less than half of the total installed capacity. The layout defined by these 99% quantiles can be seen in Fig. 3(c). It is also noteworthy that today's capacities already provide 35.5% of the benefit of transmission, if applied to this scenario. In order to find out how the benefit scales with increasing transmission capacities, ways of interpolating between today's system and the larger layouts are now defined.

Interpolation A is an upscaling of present capacities with a linear factor a . That is, for a directed link l , the limits are defined by

$$f_l^A = \min\{af_l^{\text{today}}, f_l^{99\text{Q}}\}, \quad (27)$$

where f_l^{today} represents the NTC of the link as of 2012 and $f_l^{99\text{Q}}$ those of the 99% Quantile layout.

Interpolation B involves a linear reduction of the 99% quantile capacities with factor b , that is

$$f_l^B = bf_l^{99\text{Q}}. \quad (28)$$

Interpolation C defines the capacity layout

$$f_l^C = cf_l^{\text{CQ}}, \quad (29)$$

which allows unconstrained flow for a percentage c of time, as shown by the different quantiles in Fig. 4. Here, more capacity is allocated to more transited links than to less used ones.

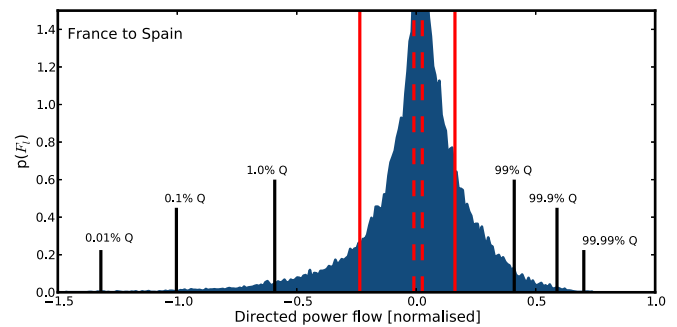


Fig. 4. Distribution of unconstrained, non-zero power flows between France and Spain, normalized to the mean load in France (see Table 1). Several low- and high-quantiles are marked for illustration. The dashed red lines represent current capacities. The solid red lines show capacities as defined by the Intermediate layout. Zero-flow events occur around 46% of the time, and are not shown. (For interpretation of the references to colour in this figure legend, the reader is referred to the web version of this article.)

Table 2

Studied layouts with their total installed transmission capacities, the required total European balancing energy E in absolute and relative terms, and the benefit of transmission β .

Layout	Total transmission capacity [GW]	E [TWh]	E (percentage of annual consumption)	Benefit β of transmission
Zero transmission	0	735	24.3%	0.0%
Present layout	73	636	21.0%	35.5%
Intermediate layout	158	539	17.8%	70.8%
99% Quantile layout	395	464	15.3%	97.6%
Unconstrained layout	840	457	15.1%	100.0%

Fig. 5 shows the average balancing energy required by all nodes for different transmission layouts, following all three interpolations. We use the larger of the NTC on each link direction as a proxy to estimate the total installed capacity shown on the x-axis.

Today's existing transmission capacity already provides a reduction in balancing energy from 24% to 21% of the annual consumption, providing 35% of the possible benefit of transmission. This is not as much as a more efficient distribution of the resources could have achieved. With the same total amount of transmission capacities, layouts B and C lead to a balancing energy of 20% of the annual consumption, with the benefit of transmission being 45%. An increase of today's total capacities by a factor of 2 in the way described by interpolations B or C, from 73 GW to 158 GW, will double the benefit of transmission to 70%, reducing the balancing energy to about 18% of the annual consumption. This new layout is between today's transmission capacities and the capacities defined by the 99% quantiles. Hence, we denote it as the Intermediate layout. It can be seen in Fig. 3(b), and its capacities are also listed in Table 3. Overall results for the Intermediate layout are presented in Table 2.

Notice that some of the capacities under the Intermediate layout are smaller than the ones in the present one. The link between Norway and Sweden, for instance, is $f_{NO-SE}^{\text{today}} = 3.90$ GW while $f_{NO-SE}^{\text{inter}} = 2.26$ GW. This is due to the fact that the Intermediate layout is presented as a reduction of the 99% quantiles, and not as an expansion of the present one.

4. Discussion: country perspectives

After having quantified how much the strengthening of the interconnectors between the countries reduces the total

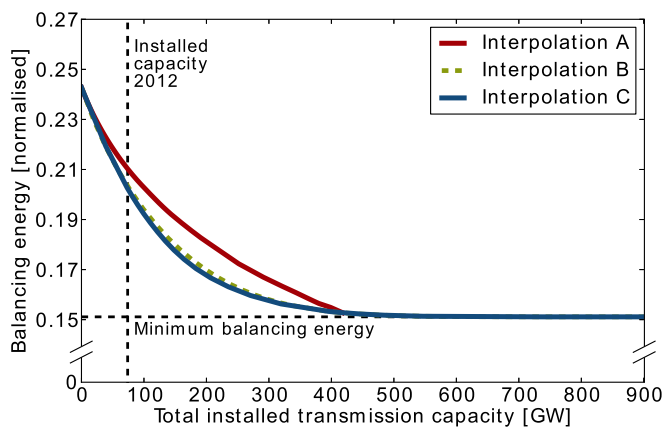


Fig. 5. Balancing energy as a function of the total installed transmission capacity for different interpolations, normalized to the total annual consumption. The vertical dashed line indicates the total installed transmission capacity as of 2012, and the horizontal dashed line the total balancing required for the unconstrained flow. Notice that the intersection with the y-axis is congruent with the results shown in Fig. 2 for the average balancing required.

balancing energy of Europe, we are now interested in what the different transmission capacity layouts imply for the import/export capabilities and the balancing power capacities of the single countries.

4.1. Limits to export and import capabilities

Let us have a look again at Table 2. Compared to the Zero transmission layout, the Unconstrained layout reduces the European balancing energy by 37.8%, from 727 TWh to 452 TWh. It is caused by the power flows from countries with an excess power generation to those with a deficit. The 37.8% can also be interpreted as the maximum capability for imports and exports. This number can not become larger since it is already based on the unconstrained transmission layout. It draws the limit to the benefit that geographical dispersion of VRES can bring to Europe. For the constrained transmission layouts the import/export capabilities are smaller. The relative reduction in balancing energy is 12.9%, 26.4% and 36.6% for the present, the intermediate and the 99% quantile transmission layouts, respectively.

So far, the reduction in balancing energy has been discussed for total Europe only. For the single countries the reduction does not need to be the same, although the average over all countries has to reproduce Europe's reduction in balancing energy. Fig. 6 illustrates the time-averaged country-specific residual loads for the different transmission capacity layouts. Apparently, some countries have better import capabilities than others. Most of the small middle and southern countries show a pronounced reduction of balancing energy from the present to the intermediate transmission capacity layout. As to the larger countries, France benefits the most from imports, and Great Britain the least. Compared to the present transmission capacity layout, the intermediate transmission layout reduces the balancing energies between 2% (for Lithuania) and 25% (for Slovenia). For the 99% quantile transmission layout the respective reductions are in the range between 17% (for Lithuania) and 37% (for Greece).

Fig. 6 also shows the country-specific average excess powers for the various transmission capacity layouts. For some countries like Great Britain, Ireland, the Netherlands, Romania, Croatia and Portugal the average excess powers turn out to be smaller than their average residual loads. With the further extension of the present transmission capacity layout, these countries will be able to export more than what they will be able to import. Other countries like Switzerland, Austria and Czech Republic will become strong importers. It is interesting to note that the stronger transmission capacity layouts quite naturally lead to stronger import/export imbalances for the countries. Please refer to [23] for an extended discussion on countries' export and import capabilities on the road to future energy systems.

4.2. Balancing power capacities

Fig. 7 shows the distributions of non-zero mismatches for three selected countries, as they change for different transmission capacity layouts. The central part of the distributions is lowered as the transmission capacity layouts become stronger. This connects nicely to the results on the reduction of average residual load and excess power, which have been discussed in the previous subsection. While the central part of the distribution, lying between -1 and $+1$ times the mean load, noticeably shrinks with increasing transmission layouts, the tails, lying below -1 and above $+1$ remain unaffected. Referring to Fig. 2(c), this implies that the 99% quantiles of the residual load and the excess power for the non-zero transmission capacity layouts are not reduced when compared to

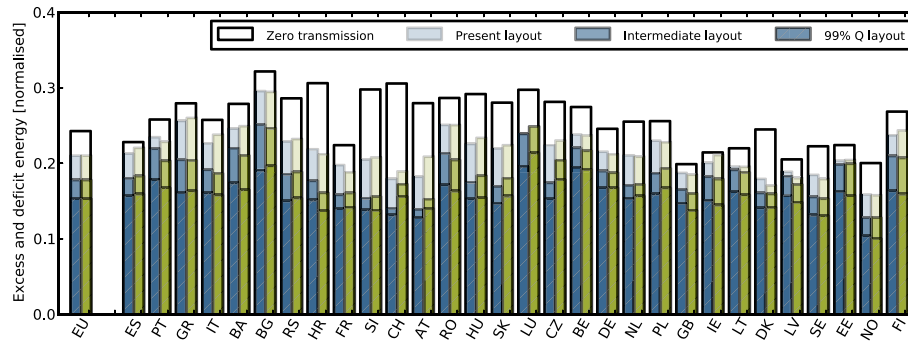


Fig. 6. Country-specific average residual loads (blue) and excess energies (green) on the Zero transmission layout, the Present layout, the Intermediate layout and the 99% Quantile layout. Residual loads and excess energies are normalized by the average load. Bars are not stacked. The optimal wind mixes d_n^W from Fig. 2(a) have been used for each country. Note, that the residual loads for the Zero transmission layout are identical to those shown in Fig. 2(b). (For interpretation of the references to colour in this figure legend, the reader is referred to the web version of this article.)

those for the zero transmission capacity layout. In other words, it appears that increased transmission does not affect the maximum balancing power, and that Europe has to keep its present dispatchable power generation capacity.

However, this would be a pre-mature conclusion. The objective of the current power flow modelling, as presented in Section 2, has been first to reduce the overall balancing energy the most using only export of excess generation, and then to determine the most localized power flow across the network.

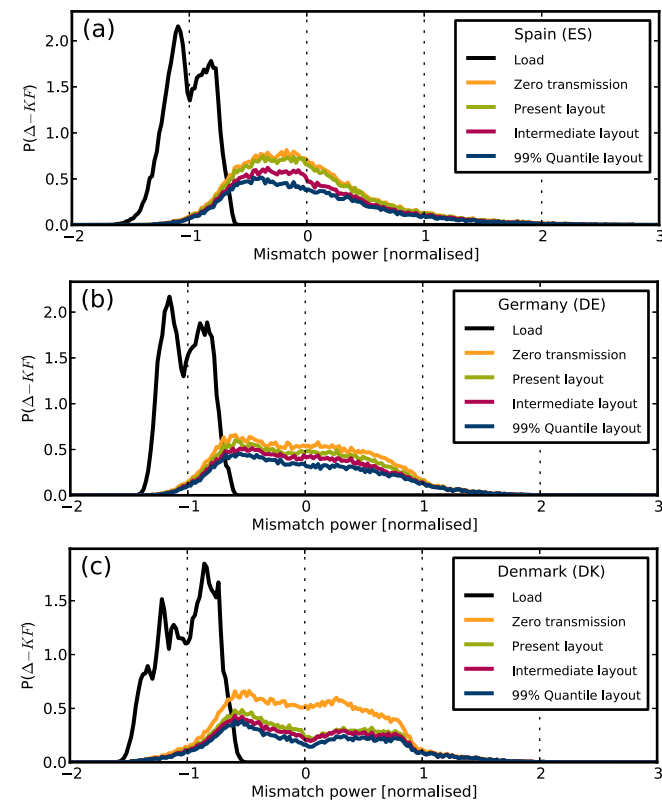


Fig. 7. Normalized non-zero distributions for residual load (below zero) and excess generation (above zero). (a) Spain, (b) Germany and (c) Denmark, with a country-specific optimal mix of wind and solar. Apart from the zero transmission scenario (orange), three layouts are shown: the Present layout (green), the Intermediate layout (purple) and the 99% Quantile layout (blue). For comparison, the distribution of the normalized load (black) is also shown. (For interpretation of the references to colour in this figure legend, the reader is referred to the web version of this article.)

The objective has not been to reduce the high quantiles of the residual load at each node of the network. In other words, the reduction of balancing power capacities has not been prioritized in the current power flow modelling. Fig. 2(c) gives an indication about how much the balancing power capacities can be reduced in principle. The first bar of this figure shows the 1% quantile of the mismatch for an aggregated Europe. With 73% of the average European load it is significantly smaller than 108%, which holds true for an average independent single country. This is also nicely visualized in Fig. 8, which shows the respective mismatch distribution for Europe with unconstrained transmission and for an average country in the zero transmission scenario. Compared to the single-country distribution, both tails of the European distribution are significantly shifted towards zero mismatch – making the mismatch distribution narrower. The explanation for this reduction in the overall balancing capacities lies in the sharing of balancing capacities between countries.

This effect of shared balancing is not taken into account in the current power flow modelling, where after import of excess renewable power the countries balance their remaining deficit fully by themselves. Shared balancing implies that countries are allowed to import part of their remaining deficit from balancing capacities of other countries, which are not fully used at the same time. This of course also leads to additional power flows. A self-consistent treatment of power-flow modelling with shared balancing capacities will not be given here. Other ways of reducing peak balancing power could include demand flexibility, the use of energy storage, and penetration of renewables larger than 100%. For the moment we will leave all of this open for future investigations.

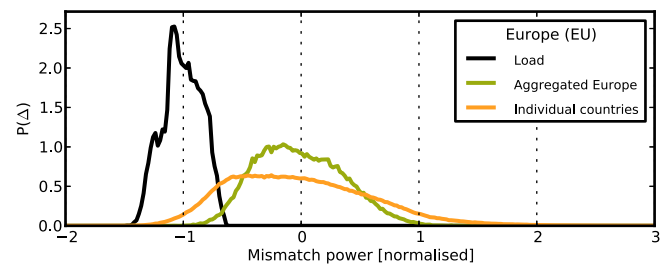


Fig. 8. Normalized non-zero mismatch distribution for Europe resulting from the unconstrained transmission scenario (green) and for an average country in the zero transmission scenario (orange). For comparison, the distribution of the normalized European load (black) is also shown. (For interpretation of the references to colour in this figure legend, the reader is referred to the web version of this article.)

5. Conclusion

We have quantified the benefit of the far-future pan-European transmission system when, by assumption, all countries have reached a 100% penetration of combined wind and solar power generation. Two extreme transmission scenarios, Zero and Unconstrained, can be treated without any power flow calculations. For the scenario with zero inter-connectors, the countries can be discussed separately. Their annual balancing energy, which is required to cover the negative mismatches between their renewable power generation and their load, depends on the wind share α_n^W of VRES power generation, becomes minimal at $\alpha_n^W \approx 0.71$ (with a small dependence on the geographical latitude), and then results to be around 24% of their annual electricity consumption. For the scenario with infinitely strong inter-connectors and no transmission losses, all country-specific mismatches can be directly aggregated into an overall European mismatch. This leads to a required balancing energy that is only 15% of the total annual European electricity consumption. The difference 24%–15% between the outcomes of the two extreme scenarios represents an upper limit on the benefit that a pan-European transmission system can provide. In other words, no transmission layout is able to further reduce the required balancing energy.

In order to estimate the benefit of transmission capacities constrained between zero and infinity, a novel modelling approach has been presented, which calculates the constrained power flows for a pan-European network. Based on highly resolved spatio-temporal weather data, it first minimizes the all-European residual load, so that as much of the overall renewable power generation is used as possible. In a second step, the square sum over all flows is minimized, leading to a very local flow pattern. This process allows us to avoid making assumptions regarding market-economic policies. This novel modelling approach reveals that an infinitely strong European transmission network should be 11.5 times as strong as today's total inter-connector capacities. A capacity layout five times as large as today's provides 98% of the benefit of transmission, which is almost as good as the infinitely strong layout for the reduction of required balancing energy. For weaker transmission networks, the relationship between the need for balancing energy and the total capacity of the transmission layout turns out to be non-linear and convex. A good compromise between these two conflicting objectives, i.e. on the one hand reducing the balancing energy as much as possible and on the other to increase the transmission capacities as little as possible, appears to be an Intermediate layout with total transmission capacities being twice as large as today's capacities. This Intermediate layout leads to a 70% benefit of transmission. Compared to the Zero transmission layout it reduces the required European balancing energy from 24% to 18% of the annual consumption. This reduction from 24% to 18% also implies that an average country participating in the pan-European transmission network can only import around a quarter of its own balancing needs, and that the remainder must come from its own balancing resources.

The presented findings have focused on the transmission needs in a fully renewable European power system. The penetration of combined wind and solar power generation has been assumed to be exactly 100%. Of course, this can be generalized to penetrations below 100%, and thus provide information on the required ramp-up of transmission needs all the way from today's penetration to the far-future 100% penetration [23]. In this respect, also a modification of the network topology should be discussed, like for example the addition of new links across the North Sea. In order to reduce the need for balancing energy further below the discussed 15% limit of the annual electricity consumption, one could look at renewable penetrations above 100% and discuss more synergies between

balancing, transmission and storage. Although outside of the scope of the present work, a cost-optimal system layout, including VRES, balancing, transmission and storage capacities, needs to be explored.

Acknowledgements

The authors thank Uffe Poulsen and Morten G. Rasmussen for insightful discussions. S.B. gratefully acknowledges financial support from O. and H. Stöcker, and G.B.A. financial support from DONG Energy and The Danish National Advanced Technology Foundation.

Appendix A

Table 3a
Interconnector capacities for different layouts.

Link	Present layout (GW)	Intermediate layout (GW)	99% Q layout (GW)	Unconstrained layout (GW)
AT \rightleftharpoons CH	0.47	2.26	5.65	14.06
	1.20	2.05	5.13	11.50
AT \rightleftharpoons CZ	0.60	3.23	8.08	15.75
	1.00	2.78	6.94	12.08
AT \rightleftharpoons HU	0.80	2.31	5.78	10.38
	0.80	3.23	8.09	19.56
AT \rightleftharpoons DE	2.00	5.27	13.17	28.33
	2.20	4.26	10.64	17.36
AT \rightleftharpoons IT	0.22	3.39	8.48	15.38
	0.28	4.10	10.25	21.55
AT \rightleftharpoons SI	0.90	1.96	4.90	7.92
	0.90	2.66	6.64	15.53
FI \rightleftharpoons SE	1.65	5.86	14.64	24.54
	2.05	4.13	10.31	15.32
FI \rightleftharpoons EE	0.35	0.98	2.45	4.28
	0.35	1.16	2.91	5.12
NL \rightleftharpoons NO	0.70	4.03	10.07	19.31
	0.70	4.20	10.50	19.94
NL \rightleftharpoons BE	2.40	2.87	7.17	12.88
	2.40	3.05	7.62	16.28
NL \rightleftharpoons GB	1.00	4.71	11.77	26.99
	1.00	5.08	12.70	25.03
NL \rightleftharpoons DE	3.00	3.59	8.98	19.10
	3.85	3.48	8.70	19.57
BA \rightleftharpoons HR	0.60	1.42	3.54	7.22
	0.60	0.91	2.28	3.85
BA \rightleftharpoons RS	0.35	0.96	2.39	4.16
	0.45	0.72	1.79	4.03
FR \rightleftharpoons BE	3.40	3.39	8.49	19.11
	2.30	3.26	8.15	13.89
FR \rightleftharpoons GB	2.00	6.03	15.07	31.20
	2.00	6.49	16.24	27.63
FR \rightleftharpoons CH	3.20	4.27	10.69	26.02
	1.10	3.94	9.84	25.90
FR \rightleftharpoons DE	2.70	6.67	16.67	35.41
	3.20	6.18	15.46	31.28
FR \rightleftharpoons IT	2.58	6.51	16.27	36.46
	0.99	7.52	18.80	40.46
FR \rightleftharpoons ES	1.30	8.39	20.98	37.67
	0.50	12.11	30.28	75.44
NO \rightleftharpoons SE	3.60	2.26	5.64	11.96
	3.90	2.18	5.46	13.57
NO \rightleftharpoons DK	0.95	1.69	4.22	8.18
	0.95	1.49	3.73	7.59
GB \rightleftharpoons IE	0.45	1.03	2.59	4.50
	0.08	0.92	2.29	4.34
PL \rightleftharpoons CZ	1.80	2.11	5.28	8.93
	0.80	2.12	5.30	11.42
PL \rightleftharpoons DE	1.10	2.67	6.69	12.87
	1.20	2.60	6.50	12.42

Table 3.b

Interconnector capacities cont. (NRL, No Realistic Limit)

Link	Present layout (GW)	Intermediate layout (GW)	99% Q layout (GW)	Unconstrained layout (GW)
PL ⇌ SE	0.00	3.23	8.07	18.51
	0.60	3.66	9.14	16.96
PL ⇌ SK	0.60	2.70	6.76	11.10
	0.50	3.39	8.49	16.79
BG ⇌ GR	0.55	2.21	5.53	14.41
	0.50	1.94	4.85	10.49
BG ⇌ RO	0.60	1.35	3.37	7.09
	0.60	1.02	2.56	5.11
BG ⇌ RS	0.45	2.03	5.08	11.09
	0.30	1.26	3.16	5.82
GR ⇌ IT	0.50	4.00	9.99	20.46
	0.50	2.66	6.66	11.69
PT ⇌ ES	1.50	2.47	6.18	12.35
	1.70	1.87	4.68	7.79
CH ⇌ DE	3.50	4.55	11.37	21.86
	1.50	4.13	10.34	16.66
CH ⇌ IT	4.17	3.64	9.10	14.92
	1.81	4.90	12.24	26.52
HR ⇌ HU	0.80	1.46	3.66	7.26
	1.20	1.10	2.76	4.89
HR ⇌ RS	0.35	0.85	2.14	3.24
	0.45	1.32	3.31	7.42
HR ⇌ SI	1.00	2.09	5.21	12.94
	1.00	1.60	3.99	7.09
RO ⇌ HU	0.70	3.07	7.68	16.10
	0.70	1.94	4.84	7.45
RO ⇌ RS	0.70	1.30	3.26	5.68
	0.50	0.79	1.98	3.82
CZ ⇌ DE	2.30	2.91	7.27	16.52
	0.80	2.58	6.44	12.49
CZ ⇌ SK	2.20	1.28	3.21	5.46
	1.20	1.74	4.34	8.76
HU ⇌ RS	0.60	1.67	4.18	6.47
	0.70	2.32	5.79	13.11
HU ⇌ SK	0.60	4.31	10.76	24.98
	1.30	3.30	8.26	13.65
DE ⇌ SE	0.60	3.93	9.83	16.70
	0.61	4.38	10.94	20.40
DE ⇌ DK	1.55	2.61	6.51	12.12
	2.08	2.77	6.92	12.94
DE ⇌ LU	0.98	0.25	0.63	0.91
	NRL	0.34	0.86	1.51
SE ⇌ DK	1.98	1.87	4.67	8.40
	2.44	1.66	4.16	7.24
IT ⇌ SI	0.16	2.18	5.45	12.26
	0.58	1.99	4.97	12.72
EE ⇌ LV	0.75	0.58	1.45	2.57
	0.85	0.67	1.68	3.08
LV ⇌ LT	1.30	0.41	1.01	1.73
	1.50	0.48	1.21	2.16

References

- [1] Jacobson MZ, Delucchi MA. Providing all global energy with wind, water, and solar power, part i: technologies, energy resources, quantities and areas of infrastructure, and materials. *Energy Policy* 2011;39(3):1154–69.
- [2] Delucchi MA, Jacobson MZ. Providing all global energy with wind, water, and solar power, part ii: reliability, system and transmission costs, and policies. *Energy Policy* 2011;39(3):1170–90.
- [3] European Photovoltaic Industry Association. Connecting the sun: solar photovoltaics on the road to large-scale grid integration. Technical report, EPIA; September 2012.
- [4] Van de Putte J, Short R. Battle of the grids. Technical report. Greenpeace International; 2011.
- [5] Cho A. Energy's tricky tradeoffs. *Science* 2010;329(5993):786–7.
- [6] Andresen GB, Rasmussen MG, Rodriguez RA, Becker S, Greiner M. Fundamental properties of and transition to a fully renewable pan-european power system. In: EPJ Web of Conferences, vol. 33; 2012. p. 04001.
- [7] Heide D, Von Bremen L, Greiner M, Hoffmann C, Speckmann M, Bofinger S. Seasonal optimal mix of wind and solar power in a future, highly renewable Europe. *Renew Energy* 2010;35(11):2483–9.
- [8] Heide D, Greiner M, Von Bremen L, Hoffmann C. Reduced storage and balancing needs in a fully renewable European power system with excess wind and solar power generation. *Renew Energy* 2011;36(9):2515–23.
- [9] Schaber K, Steinke F, Hamacher T. Transmission grid extensions for the integration of variable renewable energies in Europe: who benefits where? *Energy Policy* 2012;43:123–35.
- [10] Schaber K, Steinke F, Mühlich P, Hamacher T. Parametric study of variable renewable energy integration in Europe: advantages and costs of transmission grid extensions. *Energy Policy* 2012;42:498–508.
- [11] Rasmussen MG, Andresen GB, Greiner M. Storage and balancing synergies in a fully or highly renewable pan-european power system. *Energy Policy* 2012;51:642–51.
- [12] Steinke F, Wolfrum P, Hoffmann C. Grid vs. storage in a 100% renewable Europe. *Renew Energy* 2013;50(0):826–32.
- [13] Van Hulle F, et al. Integrating wind. Developing Europe's power market for the large-scale integration of wind power: executive Summary. Technical report. European Wind Energy Association; 2009.
- [14] Buijs P, Bekaert D, Cole S, Van Hertem D, Belmans R. Transmission investment problems in Europe: going beyond standard solutions. *Energy Policy* 2011;39(3):1794–801.
- [15] Tröster E, Kuwahata R, Ackermann T. European grid study 2030/2050. Technical report. Energynautics GmbH; 2011.
- [16] European Transmission System Operators. Ten-year network development plan 2012. Technical report. ENTSO-E; 2012.
- [17] Zugno M, Pinson P, Madsen H. Impact of wind power generation on european cross-border power flows. *IEEE Transac Power Syst* 2012.
- [18] Corcoran BA, Jenkins N, Jacobson MZ. Effects of aggregating electric load in the United States. *Energy Policy* 2012;46:399–416.
- [19] Wollenberg B, Wood A. Power generation, operation, and control. John Wiley & Sons; 1996.
- [20] Van Hertem D, Verboomen J, Purchala K, Belmans R, Kling WL. Usefulness of DC power flow for active power flow analysis with flow controlling devices. In: The 8th IEEE international conference on AC and DC power transmission. IET; 2006. p. 58–62.
- [21] Lehmkoetter C. Security constrained optimal power flow for an economical operation of FACTS-devices in liberalized energy markets. *IEEE Transac Power Deliv* 2002;17(2):603–8.
- [22] Mattingley J, Boyd S. CVXGEN: a code generator for embedded convex optimization. *Optim Eng* 2012;1–27.
- [23] Becker S, Rodriguez RA, Andresen GB, Schramm S, Greiner M. Transmission grid extensions during the build-up of a fully renewable European electricity supply. Review to Energy. Available at: <http://arxiv.org/abs/1307.1723>.
- [24] European Transmission System Operators. Indicative values for net transfer capacities (NTC) in continental Europe. Technical report. ENTSO-E; 2011.
- [25] Skog JE, Koreman K, Pääjärvi B, Worzyk T, Andersröd T. The NorNed HVDC cable link: a power transmission highway between Norway and the Netherlands. Technical report. ABB; 2007. Online, retrieved July 2013.
- [26] BritNed Development Limited. BritNed construction. <http://www.britned.com/>. Online, retrieved July 2013.